A Comparison of Near-Infrared Diode Laser Techniques for Airborne Hygrometry

JOEL A. SILVER AND DAVID CHRISTIAN HOVDE

Southwest Sciences, Inc., Santa Fe, New Mexico

(Manuscript received 6 December 1995, in final form 1 July 1996)

ABSTRACT

High-frequency wavelength modulation spectroscopy and dual beam absorption noise canceler methods are compared for near-infrared laser detection of moisture at levels relevant to airborne hygrometry. Both techniques exhibit sensitivities exceeding −85°C frost point, with subsecond time response. The application of these techniques to airborne hygrometric instrumentation is discussed.

1. Introduction

The measurement of local concentrations of water vapor in the troposphere and lower stratosphere plays an important role in many aspects of atmospheric research (Stephens and Slingo 1993) and is of importance for safety assessment in commercial aviation (Hills and Fleming 1994). A wide variety of methods exists for local measurement of humidity or dewpoint or frost point. These include thin-film capacitive sensors, chilled mirrors, near-infrared (IR) diode laser absorption, carbon hygristors, fiber optic sensors, midinfrared diode laser or broadband absorption, lithium chloride sensors (dewcells), piezoelectric sensors, sling psychrometers, mass spectrometers, and UV absorption (typically Lyman-α or photofragment fluorescence). Many of these instruments exhibit a critical drawback for airborne meteorological sensing such as hysteresis, slow time response, insufficient dynamic range, or poor sensitivity (McKay 1978). A recent comprehensive review of airborne hygrometer technologies suitable for commercial aviation applications (Hills and Fleming 1994) concludes that only the first three methods in the above list meet the requirements for a commercial aviation sensor. Near-infrared diode laser absorption spectroscopy measures the water vapor concentration directly with sensitivities matching or exceeding those of the chilled mirrors, but with much faster (less than 1 s) time response.

The research reported in this paper compares two approaches to near-infrared diode laser absorption with the potential for improved overall capabilities for monitoring atmospheric water vapor, as compared with any other available hygrometer. The two approaches are high-frequency wavelength modulation spectroscopy (WMS) and dual beam spectroscopy using newly developed noise cancellation (NC) electronic circuitry. The former method shifts the detection bandwidth to a high-frequency regime where excess $(1/f)$ laser noise becomes negligible. WMS methods produce a derivative-like signal line shape and require only a single optical beam. The NC method uses dual beams (sample and reference) to identically cancel all noise sources except those arising from within the absorption path. In contrast to WMS, the NC directly provides the absorption line shape. This can be advantageous for systems in which the pressure varies widely because the line shape and peak height change with pressure. Both methods permit the development of a self-calibrated monitoring system with very wide dynamic range and fast time response and are compatible with fiber optics.

To compare these approaches, a 1393-nm near-infrared diode laser operating near room temperature was used to measure water vapor concentrations within a compact single-pass absorption cell. Calibrations were made against a commercial chilled mirror hygrometer over a range of frost points from −3° to near −80°C. Calibrated moist flows were generated by mixing measured flows of dry nitrogen with lab air or water vapor. The performance, accuracy, and time response for both detection methods are assessed and compared. The application of both techniques for airborne operation, including the use of fiber optics, is discussed.

2. Near-infrared diode laser absorption

The WMS and NC methods probe narrow absorption features of water vapor. Unlike low-resolution absorption methods, for which the absorbance represents the average cross section within some instrumental function, the near-infrared diode laser instrument measures the absorbance at essentially a single optical frequency.

Corresponding author address: Joel A. Silver, Southwest Sciences, Inc., 1570 Pacheco Street, Suite E-11, Santa Fe, NM 87505.

Governed by Beers' law, the optical absorbance $\alpha(\nu)$ is expressed as

$$\alpha(\nu) = \ln\left(\frac{I_0}{I}\right), \tag{1a}$$

where

$$\alpha(\nu) = \sigma(\nu)Nl = \frac{\sigma(\nu)P_{\mathrm{H_2O}}l}{kT_{\mathrm{gas}}}. \tag{1b}$$

The absorption cross-sectional line shape is $\sigma(\nu)$, ν is the laser frequency, N is the number density of water, P is the water vapor partial pressure, and l is the absorption pathlength. The Boltzmann constant is k, and T_{gas} is the gas temperature in kelvins; I_0 is the initial light intensity, and I is the intensity after passage through the absorbing gas. Measurement of absorbance provides the water vapor partial pressure, which can be readily converted to frost point.

The line shape function $\sigma(\nu)$ is pressure and temperature dependent. It changes from a Gaussian profile (Doppler low pressure limit) to a Lorentzian shape at high pressures. For atmospheric pressures typical of the upper troposphere, a Voigt line shape (convolution of Gaussian and Lorentzian) must be used for an accurate representation of the line shape.

The major factors limiting optimum detection sensitivity with absorption techniques are source excess $(1/f)$ noise and the formation of accidental optical interference fringes (etalons). Due to scattering or stray reflections, a small amount of light follows a different path than the main beam to the detector. Since the laser radiation is coherent, optical interference occurs and shows up as regularly spaced fringes in the absorption spectrum. Fringe spacings are often similar to the gas line width. These etalons can be minimized with careful optical design, as well as by active suppression techniques (Silver and Stanton 1988). With excess noise and unwanted etalons removed, near quantum-limited detection levels approaching 10^{-7} fractional absorbance can be achieved (Bomse et al. 1992 and references therein).

a. Water vapor spectroscopy in the near-infrared

The spectral region accessed by the near-IR diode laser contains many water vapor absorption bands that are overtones or combinations of fundamental modes (HITRAN database; Rothman et al. 1992). The region of greatest line strengths (mostly the $\nu_1 + \nu_3$ band) lies between 1340 and 1395 nm and is about one order of magnitude weaker than the strongest infrared fundamental lines. The laser used in this study accesses the $3_{0,3} \leftarrow 2_{0,2}$ rotational transition in the $\nu_1 + \nu_3$ vibrational band at 1392.53 nm. This line was selected for its combination of good line strength and clear separation from other spectral features due to water and other atmospheric gases. From measured values of the spectral parameters (Delaye et al. 1989; Arroyo and Hanson 1993; Toth 1994; Silver et al. 1995), highly accurate absorption cross sections can be calculated for all expected temperatures and pressures.

b. Near-infrared diode lasers

The light source is a distributed feedback InGaAsP diode laser operating in the wavelength region near 1393 nm. The distributed feedback structure guarantees single-mode operation. Coarse tuning of the laser wavelength is accomplished by varying the laser temperature using an internal thermoelectric cooler. High-resolution wavelength tuning is obtained by varying the laser injection current. The laser used here has a temperature tuning rate of approximately 0.08 nm $^{\circ}C^{-1}$, so that operating temperatures of -20° to $+40^{\circ}$C result in a tuning range of about 4.8 nm (750 GHz). Absolute wavelength calibration of the laser is achieved using a wavemeter in combination with direct measurements of the high-resolution water vapor spectrum, where line positions as determined from the HITRAN database can be used to fit the observed patterns of lines. The absolute current tuning rate as the laser scans across the spectral feature is determined with a spectrum analyzer (300-MHz free spectral range confocal etalon). In this near-infrared spectral region, the laser is detected by a room temperature InGaAs photodiode.

c. WMS detection

WMS allows measurement of weak optical absorbances by shifting the detection band to high frequencies where laser excess $(1/f)$ noise is unimportant to achieve fractional absorption sensitivities near the shot-noise limit (approximately 10^{-7}) for both near- and midinfrared diode lasers (Bomse et al. 1992). Field measurements using WMS routinely maintain minimum detection absorbances of 10^{-5} or better (1-Hz bandwidth) for extended (many months) operation.

To implement WMS, a small sinusoidal modulation at frequency f is superimposed on the diode laser injection current. This current modulation produces a modulation of the laser wavelength since wavelength is tuned by changing the current. The amplitude of the current modulation is chosen so that the induced wavelength modulation is comparable to the width of the spectral feature under study. Absorption by the target gas converts the laser wavelength modulation to an amplitude modulation that induces ac components in the detector photocurrent. A lock-in amplifier detects the second harmonic $(2f)$ component of the modulation frequency of this ac signal. In the limit where the wavelength modulation amplitude is small compared with the spectral feature line width, the resulting processed signal is exactly the second derivative with respect to wavelength of the direct transmission spectrum. In reality,

the optimum amplitudes are much larger and the line shapes are only derivative-like.

For $\alpha < 0.2$, the WMS signal is directly proportional to the absorbance,

$$\text{Signal} = CI_0\alpha(\nu)f_{\text{WMS}}, \tag{2}$$

where C is a system electronic calibration factor. The factor f_{WMS} is an additional term introduced by WMS detection and is a function of the amplitude of the high-frequency modulation. For optimum sensitivity where the signal is defined as the $2f$ peak-to-trough height, f_{WMS} is approximately 0.6, a value that for selected lines can show less than 5% variation at a given pressure over the range of expected temperatures. Both the cross section and the WMS factor are readily evaluated from spectral parameter and experimental calibration data. More detailed descriptions of WMS methods can be found in Silver (1992) and Bomse et al. (1992).

d. Noise canceler circuit

The absorption line shape can be directly measured by scanning the laser and suppressing the $1/f$ noise using an electronic noise cancellation circuit (Hobbs 1991; Haller and Hobbs 1991). From the measured absorbance, known pathlength, and computed cross-sectional line shape, the number density is accurately obtained [see Eq. (1)]. The NC works on the principle that when an optical beam splitter divides the laser light into two beams, each beam has the same (common mode) noise spectrum characteristic of the light source. The two beams are detected on separate sample and reference photodetectors. If the amplitudes of the sample and reference beam photocurrents can be made equal, then their difference is free of common mode noise. While this technique has been in use for some time, the circuit described by Hobbs uses an especially simple scheme to equalize the photocurrents. Instead of optically balancing the photocurrents, the reference leg is intentionally made stronger than the sample leg. The balance is achieved electronically by dividing the reference current using a transistor pair, then subtracting this fraction of the reference photocurrent from the signal photocurrent. Shot noise limited sensitivity has been demonstrated (Haller and Hobbs 1991).

3. Experimental

The near-IR diode laser apparatus is shown in Fig. 1. The major subsystems of the apparatus are the diode laser and its control electronics, the optical path, a pressure-controlled sample cell, controlled moisture flow generation, and the detectors and associated signal processing. For the WMS setup, the laser output is directly focused across the sample cell; the NC uses a fiber optic cable to transfer radiation to the cell and to the reference detector.

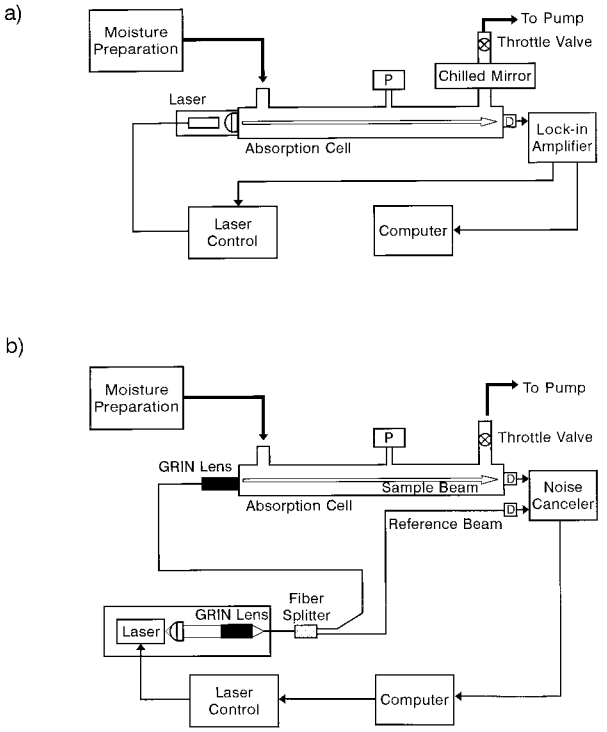

FIG. 1. Schematic of experimental apparatus used for (a) WMS detection and (b) electronic noise canceler. Photodetectors are labeled as "D."

a. Optical setup

While laser modules incorporating an optical isolator, thermoelectric cooler, thermistor, and output single-mode fiber pigtail are available, they have an unacceptable level of residual water vapor within the laser package. This moisture produces a background signal that can be 100 times larger than the smallest anticipated atmospheric signals. Although the NC removes most of this common-mode signal in the packaged module, it limits the resulting dynamic range of the device.

Our laser is packaged in a three-pin TO-46 can with the cover plate removed and is held by a thermoelectrically cooled, copper block. The laser and mounting hardware are placed in a compartment filled with 1390 mb of dry nitrogen to eliminate any water vapor signal from within the short optical path in the housing. For the WMS experiments, the laser unit is directly attached to the sample cell. The collimating lens is only 1 mm from the laser, so that optical interference fringes formed by these elements have a free spectral range of approximately 5 cm^{-1} and appear as a flat background over the few-tenths wavenumber width of the spectrum. With the NC, the laser beam is launched into a single-mode fiber using an antireflection-coated gradient index (GRIN) lens some 25 cm from the laser. The optical fiber is connected to a polarization insensitive fiber splitter, with one leg connected to the reference detector and the other leg connected to a vacuum-tight GRIN lens at

the entrance to the sample cell. The NC circuit board is placed directly behind the end flange. The use of optical fibers facilitates variable temperature studies by allowing the sample cell to be placed (remotely from the laser and data acquisition hardware) in a commercial freezer at −30°C.

A small residual water vapor signal in the NC was traced to the difference between the water vapor pressure-path product inside the sample and reference detectors. (This highlights the extremely sensitive nature of this technique because the detectors are packaged with less than a 1-mm air gap between the entrance window and the photodiode.) This residual signal disappeared when the detectors were cooled, as expected from the strong dependence of water vapor pressure on temperature.

b. Gas sampling system

As illustrated in Fig. 1, 0.5-m-long electropolished stainless steel cells fitted with temperature and pressure sensors are used to simulate trace moisture levels at various pressures and temperatures that might be encountered by an airborne hygrometer. After passing once through the sample cell, light is collected on a 3-mm-diameter InGaAs photodiode epoxied into the end flange at an angle to minimize etalon formation. Measured power at the detector is 2.8 mW. Care was taken to minimize leaks [less than 4×10^{-3} (STP) cm^3 min^{-1}] that would contaminate measurements at low moisture levels. A butterfly flow control valve throttles the pumping speed to maintain a constant pressure in the sample cell. As a result, cell flush times varied during the experiments, but no effect of flow rate on signal is observed. The WMS diode laser measurements were compared directly to frost point readings obtained using a Buck Research CR-1L liquid-nitrogen-cooled chilled mirror hygrometer positioned in the downstream flow. The Buck instrument is capable of frost points to −119.5°C.

Controlled humidity levels were generated by combining metered flows of room air and dry nitrogen. The humidity level in the lab air was measured with a wet bulb–dry bulb sling psychrometer, corrected for ambient pressure. Dry nitrogen was obtained from the boil-off of a liquid nitrogen cylinder that was passed through a commercial in-line purifier with a stated impurity level of less than 2 parts per billion.

c. WMS electronics

Commercially available electronic instrumentation is used to implement WMS detection here. A digital lock-in amplifier is used to generate the $f = 48.18$-kHz modulation sine wave. The computer programmable D/A output of the lock-in provides a voltage ramp used to sweep the laser wavelength. These two signals (modulation and ramp) are added and sent to the laser controller's modulation input.

The photocurrent is dropped across a 50-ohm load resistor. The ac component of this voltage is fed to the input of the lock-in to measure the $2f$ WMS signal. The dc signal (3-kHz low-pass filter), which is proportional to the laser intensity I_0, is preamplified and recorded by an A/D input of the lock-in. Normalization of the WMS signal to I_0 is critical to account for any variation of laser power on the detector. The origin of these variations includes changes in laser output power as the injection current is swept, optical misalignment, vibrations, obscuration or scattering of the transmitted beam, and contamination of the optics. Even severe I_0 attenuations (greater than 95%) will have little or no effect on the measured concentrations for this type of setup. The chilled mirror output voltage is recorded by a second A/D input. A laptop computer controls all the lock-in functions and reads all data from the lock-in via a GPIB (IEEE-488) interface. Spectral scans of 800 points are acquired with an effective bandwidth of 3 Hz.

d. Noise canceler electronics

A noise canceler circuit was wired following the design of Hobbs (1991), with the addition of instrumentation amplifiers for separately measuring the sample and reference photocurrents. An op-amp was the dominant white noise source, with a noise level equivalent to an optical absorbance of 2×10^{-5} in the 10-kHz bandwidth of a single scan. Signal-to-noise improvements obtained by coaveraging were limited because back reflections within the fibers introduced etalons that limited the noise floor of the coadded scans.

The laser current was ramped to achieve an 18-GHz laser frequency scan. Software developed in-house controlled the clock rate (20 μs per current step) and number of points (256) in the scan. The NC output, sample (I_0) and reference photocurrent signals, and a voltage proportional to sample pressure were digitized synchronously with the laser current ramp. These signals were stored to disk for postprocessing.

4. Results

a. WMS results

A series of measurements of water vapor were performed by varying the room air flow into the cell with a fixed flow of nitrogen. Both the chilled mirror and laser responded linearly to the flow settings. Figure 2 is a plot of the laser WMS signal versus the chilled mirror measurements converted to partial pressure of water vapor in the cell. For comparison, the corresponding frost points are displayed along the top of the graph. A linear least squares fit to this curve shows that the WMS signal is linear, with virtually no offset, over water concentrations corresponding to frost points ranging

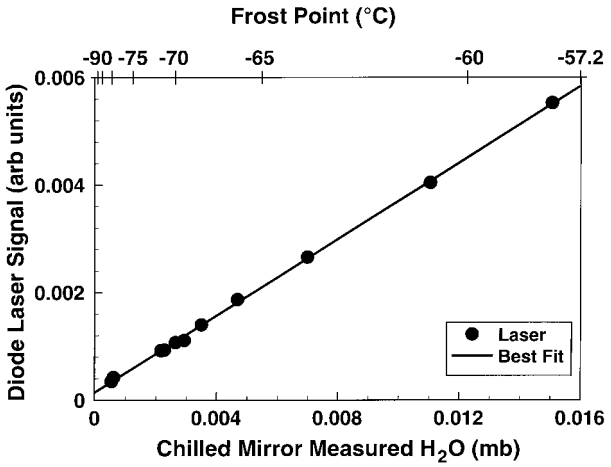

FIG. 2. Comparison of chilled mirror to diode laser signals.

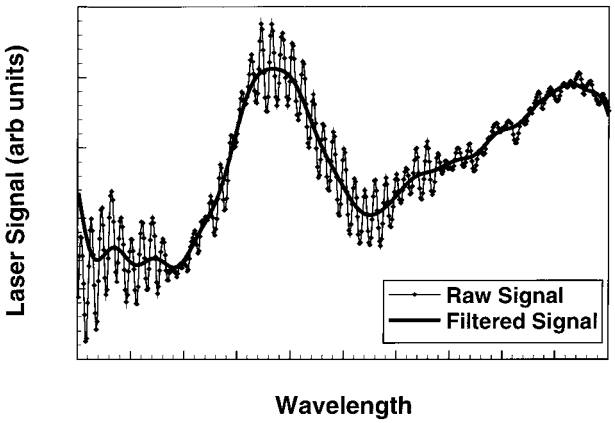

FIG. 3. Water vapor spectrum at −71.3°C frost point.

from −58° to below −80°C. The linear regression coefficient r^2 for these data is 0.99. Measurements of large concentrations of water vapor (frost points near 0°C) exhibit excellent signal-to-noise ratios and a response consistent with a linear extrapolation of the lower concentration measurements.

Figure 3 shows a raw WMS spectrum of water vapor at a frost point of −71.3°C. As seen in this figure, the water spectrum exhibits a good signal-to-noise ratio even before processing. The fluctuations in the data are not random noise but correspond to a residual high-frequency etalon arising from the detector-to-lens (or detector-to-laser) separation. The equivalent fractional absorbance of this etalon is 1.3×10^{-4}.

A wide variety of signal processing techniques have been discussed in the literature in relation to diode laser absorption analysis. They range from fast transient digitization with coadding scans to digital signal analysis methods, including optimal or matched filtering and multilinear regression techniques (Werle 1994; Press et al. 1992). Figure 3 also shows the result of applying an optimal filter to the raw data. This approach, or, alternatively, performing a multilinear regression using a stronger ''reference'' spectrum to the filtered data, results in a signal-to-noise (S/N) ratio of approximately 16. This corresponds to a minimum detectable frost point (SNR = 1, 3-Hz bandwidth) of −89°C. The equivalent fractional absorbance of this limit is approximately 2×10^{-5}. Significant improvements in sensitivity are possible because the limiting factor currently is an etalon and not the laser shot noise.

Time response of the laser and chilled mirror to abrupt changes in frost point were studied. These changes in water vapor concentration are made by rapidly switching the flow of room air from high to low or low to high. Figure 4 illustrates one set of measurements where the frost point changes from −54° to −66°C. The vertical line denotes when the flow change begins. The laser smoothly achieves 90% of the final value in 3.3 s. In contrast, the chilled mirror first undershoots the final result by 65%, then overshoots it by 70% before stabilizing after an elapsed time of 56 s. Similar results are obtained for low-to-high (−72° to −56°C) transitions. The nominal flush time (τ) of the cell based on its volume (0.33 L) and the pumping speed (15 L min^{-1}) is just 1.3 s. The observed laser response matches that expected from this flush time (3τ).

The ultimate limitation to time response using WMS detection is the demodulation frequency. Because the present noise limit is optical fringes, not white noise, the S/N ratio does not degrade as the square root of the bandwidth when the bandwidth is increased. For practical hygrometer systems, the useful response time is in milliseconds, comparable with Lyman-α hygrometers. In addition to its fast time response, the laser-based method provides absolute measurements of water vapor over long time periods.

To assess how much better WMS might do at higher frequencies, a spectrum analyzer was used to measure the power spectral density of the laser. As with other

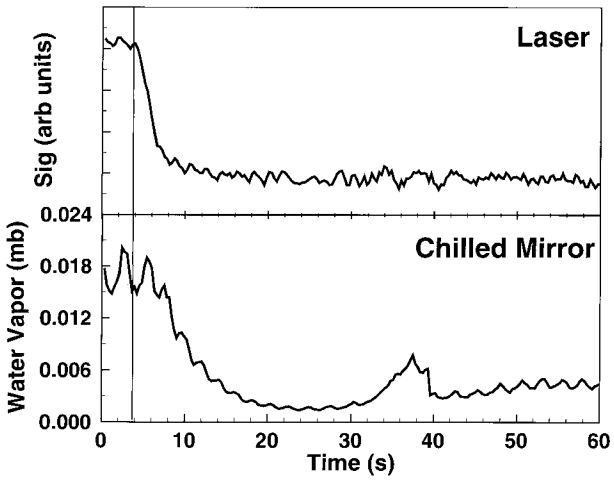

FIG. 4. Time response of laser and chilled mirror hygrometer (CR-1L) to a rapid decrease in moisture content.

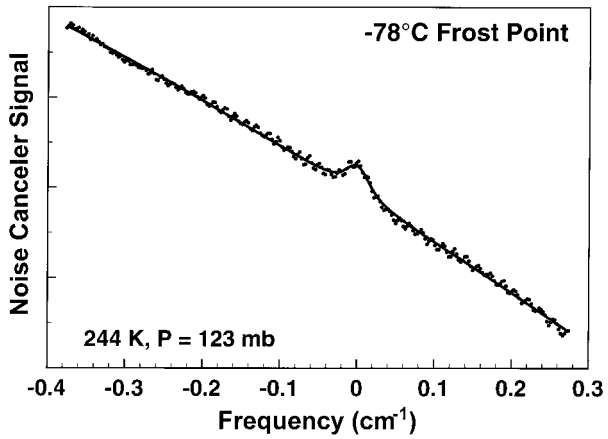

FIG. 5. Sample noise canceler spectrum of water vapor (·····) and best fit (———).

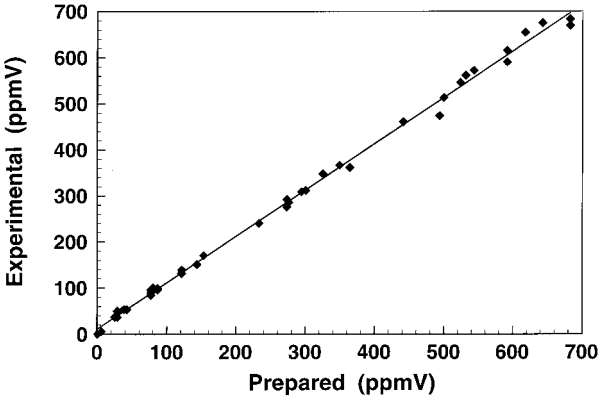

FIG. 6. Measured vs prepared mixing ratios of moisture using the noise canceler.

near-IR lasers we have used, this laser is quiet: excess $(1/f)$ noise is low and drops off at fairly low frequencies compared to lead salt or AlGaAs lasers we have observed. At $2f$ (96.4 kHz), the noise is -131 dB below the dc level and decreases another 11 dB at frequencies in the 2–20-MHz range, where high-frequency WMS (or two-tone FMS) detection methods are usually used for optimal sensitivity. This noise level corresponds to a minimum detectable absorbance of 8×10^{-8} in a 1-Hz bandwidth, which is equal to a -115°C frost point for a 50-cm optical path. As noted earlier, the current limit to sensitivity is determined by unwanted etalons. However, we anticipate a detection level of 1×10^{-6} (-104°C) is possible in a flight-worthy instrument where active etalon suppression and greater than or equal to 2-MHz detection frequencies are used.

b. Noise canceler results

The NC spectral line shapes are recorded at 38 calibrated humidity levels between 0.8 and 682 ppmv (parts per million by volume) at total pressures ranging from 66.7 to 1000 mb and temperatures from $-30°$ to $+30$°C. The spectra are fit by multilinear regression methods to a normalized Voigt line shape plus a cubic background function. Figure 5 shows an example of such a fit to a spectrum obtained at a pressure of 123 mb and a temperature of -29°C. As with the WMS experiments, high-frequency etalon fringes are present in the raw data, but the fit is well determined. The mixing ratio derived from the optical measurement is 6.2 ± 0.25 ppmv, which corresponds to a frost point of -78°C. The minimum detectable water vapor concentration under these conditions is 1 ppmv (-89°C frost point), demonstrating the capability of the NC to achieve sensitivities (S/N = 1) below -90°C with active etalon reduction.

The global fit of our experimentally determined water vapor mixing ratios to the prepared values is shown in Fig. 6. The solid line is a best linear fit. This graph shows the excellent linearity, dynamic range, and S/N of this laser-based measurement. Additional data near 10 000 ppmv also fall on this line. A small intercept can be attributed to electronic offsets. These data encompass four orders of magnitude in mixing ratio. Except for a preamplifier gain that was reduced from its typical value of 5 to 1 at the highest signal levels, the data were taken with a single set of electronic settings using a 12-bit D/A converter.

5. Discussion

Using high-frequency wavelength modulation spectroscopy or dual beam electronic noise cancellation, diode laser absorption offers a combination of accuracy, sensitivity, and time response that is unmatched by any other method for water vapor measurement. Wavelength modulation detection of water vapor is linear over the concentration range studied, with a demonstrated sensitivity limit (SNR = 1, 3-Hz bandwidth, 0.5-m path) of -89°C frost point, based on comparisons with the liquid-nitrogen-cooled mirror. Time response was superior to the chilled mirror and was limited only by the gas flow time through the absorption cell. The NC achieves similar performance levels in a flexible fiber optic instrument. The NC approach accurately recorded the absorption line shapes over a wide range of temperatures and pressures. Water vapor frost points as low as -78°C are readily detected, and a detection limit of -89°C frost point was estimated at 123 mb and 244 K. Even at the current detection limits, still lower frost points should be achievable at the lower temperatures to be encountered near the tropopause. The results of our investigation in conjunction with our prior experience (Silver and Stanton 1987; Silver and Hovde 1994) show that these methods could readily be applied to the development of compact commercial airborne hygrometers.

Although detection sensitivities are about equal in the laboratory, it is our opinion that the WMS approach is

the more viable choice for a diode-laser-based instrument at the current time. This conclusion arises from the fact that the dual beam NC approach requires a reference path free of moisture—a requirement that can be easily met only with an optical fiber. Yet existing fiberized laser housings contain too much internal moisture, so that a purged free space coupling would be required. Maintaining the alignment of such a coupling is difficult under the conditions of vibration and temperature variation found aboard research aircraft.

Both methods have similar time response and sensitivity. For an external (open) path, the NC signal is simpler to model, so it should provide greater accuracy. However, open paths are much more likely to gather ice, dust, and dirt, which reduce the transmission in the sample path and degrade the performance of the NC, resulting in higher noise levels. The NC approach will require more frequent maintenance. Modeling the WMS method requires careful calibration of the modulation amplitude relative to the line width; accuracy will be reduced by fluctuations in temperature and pressure. Sampling air into a closed path that can be carefully pressure- and temperature-controlled permits WMS methods to be applied with accuracy equal to that of the NC approach, but the interaction of moisture with the cell walls will limit the use of sampling systems to regions of relatively high moisture content.

Acknowledgments. This work was sponsored by the National Aeronautics and Space Administration under Contracts NAS1-20161 and NAS7-1360.

REFERENCES

Arroyo, M. P., and R. K. Hanson, 1993: Absorption measurements of water vapor concentration, temperature and line-shape parameters using a tunable InGaAsP diode laser. *Appl. 0pt.,* **32,** 6104–6116.

Bomse, D. S., A. C. Stanton, and J. A. Silver, 1992: Frequency modulation spectroscopy for trace species detection: Experimental comparison of methods. *Appl. Opt.,* **31,** 718–731.

Delaye, C., J.-M. Hartmann, and J. Taine, 1989: Calculated tabulations of H_2O line broadening by H_2O, N_2, O_2, and CO_2 at high temperature. *Appl. Opt.,* **28,** 5080–5087.

Haller, K. L., and P. C. D. Hobbs, 1991: Double beam laser absorption spectroscopy: Shot noise-limited performance at baseband with a novel electronic noise canceller. *Proc. SPIE, Optical Methods for Ultrasensitive Analysis: Techniques and Applications,* Los Angeles, CA, SPIE, 298–309.

Hills, A. J., and R. J. Fleming, 1994: Commercial aviation sensing humidity sensor evaluation phase. Final Rep. to FAA, 149 pp. [Available from 800 Independence Ave. SW, Washington, DC 20591.]

Hobbs, P. C., 1991: Reaching the shot-noise limit for $10. *Opt. Photonics News,* **2**(4), 17–23.

McKay, D. J., 1978: A sad look at commercial humidity sensors for meteorological applications. Preprints, *Fourth Symp. on Meteorological Observations and Instrumentation,* Denver, CO, Amer. Meteor. Soc., 7.

Press, W. H., S. A. Teukolsky, W. T. Vettering, and B. P. Flannery, 1992: *Numerical Recipes in C.* Cambridge University Press, 671–673.

Rothman, L. S., and Coauthors, 1992: The HITRAN molecular database: Editions of 1991 and 1992. *J. Quant. Spectrosc. Radiat. Transfer,* **48,** 469–507.

Silver, J. A., 1992: Frequency modulation spectroscopy for trace species detection: Theory and comparison among experimental methods. *Appl. Opt.,* **31,** 707–717.

——, and A. C. Stanton, 1987: Airborne measurements of humidity using a single-mode Pb-salt diode laser. *Appl. Opt.,* **26,** 2558–2566.

——, and ——, 1988: Optical interference fringe reduction in laser absorption experiments. *Appl. Opt.,* **27,** 1914–1916.

——, and D. C. Hovde, 1994: Near-infrared diode laser airborne hygrometer. *Rev. Sci. Instrum.,* **65,** 1691–1694.

——, D. J. Kane, and P. S. Greenberg, 1995: Quantitative species measurements in microgravity flames with near-IR diode lasers. *Appl. 0pt.,* **34,** 2787–2801.

Stephens, G., and A. Slingo, 1993: The importance of upper tropospheric water vapor for climate. Preprints, *Eighth Symp. on Meteorological Observations and Instrumentation,* Anaheim, CA, Amer. Meteor. Soc., J113–J119.

Toth, R. A., 1994: Extensive measurements of $H_2\,{}^{16}O$ line frequencies and strengths: 5750 to 7965 cm^{-1}. *Appl. Opt.,* **33,** 4851–4867.

Werle, P., 1994: Signal processing strategies for tunable diode laser spectroscopy. *Proc. SPIE, Tunable Diode Laser Spectroscopy, Lidar, and DIAL Techniques for Environmental and Industrial Measurements,* Atlanta, GA, SPIE, 19–30.